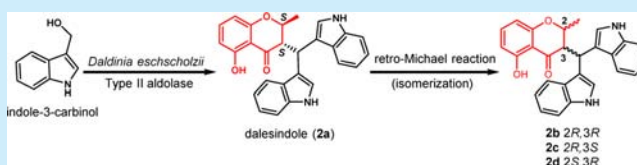


Gene-Inspired Mycosynthesis of Skeletally New Indole Alkaloids

Li Ping Lin,^{†,‡} Peng Yuan,[†] Nan Jiang,[§] Ya Ning Mei,^{||} Wen Jing Zhang,[†] Hui Min Wu,[†] Ai Hua Zhang,[†] Jiang Ming Cao,[†] Zheng Xin Xiong,[§] Ye Lu,[‡] and Ren Xiang Tan^{*,†}[†]State Key Laboratory of Pharmaceutical Biotechnology, Institute of Functional Biomolecules, Nanjing University, Nanjing 210093, China[‡]Jiangsu Center for Research & Development of Medicinal Plants, Institute of Botany, Jiangsu Province and Chinese Academy of Sciences, Nanjing 210014, China[§]School of Pharmacy, Nanjing Medical University, Nanjing 210029, China^{||}Department of Clinical Laboratory, the First Affiliated Hospital of Nanjing Medical University, Nanjing 210029, China

Supporting Information

ABSTRACT: Dalesindole, an antibacterial and anti-inflammatory indole alkaloid with an undescribed carbon skeleton, was stereoselectively constructed by *Daldinia eschscholzii* through class II aldolase catalyzed Michael addition of fungal chromone with 3,3'-diindolylmethane (DIM) formed in situ from indole-3-carbinol (I3C) under catalyses of monooxygenase and 8-amino-7-oxononanoate synthase (AONS). Dalesindole isomerizes via a retro-Michael reaction to give stereoisomers with bioactivities. The work provides an access to new bioactive hybrids of fungal oligoketide with microbially decorated exogenous chemistry.



Carbon–carbon (C–C) bond formation is a key step toward organic molecules, and knowledge about natural product biosynthesis indicates that such covalent bonds can form with regio- and stereoselectivity under physiological conditions, namely, at neutral pH and ambient temperature in aqueous solution without protecting groups.^{1,2} The bonding accommodates an unforeseeable diversity of natural products in the ecosystem.^{3,4} Among organic molecules, indole alkaloids have found widespread applications in the pharmaceutical industry and agrochemical manufacture.^{5,6} Chemical synthesis of this alkaloid family remains an important research topic, but are challenged by the inevitable utilization of toxic/expensive reagents and continuous requirement for chemical space expansion.^{7,8} To cope with this frustration, precursor-directed biosynthesis⁹ and the mutasynthetic approach¹⁰ have been established. Moreover, the silent fungal Pictet–Spenglerase gene has been identified and activated to synthesize an array of unpredictable indole alkaloids with fungal oligoketide motifs.¹¹ These observations highlight that some fungi could be efficient producers of indole alkaloids with unforeseeable skeletons and bioactivities.

Daldinia eschscholzii IFB-TL01, a fungus residing originally in mantis (*Tenodera aridifolia*) guts, generates no alkaloid, but instead produces structurally diverse and biologically active aromatic polyketides including the immunosuppressive dalesconols A and B.¹² Biosynthetic attention to dalesconols A and B has indicated that the fungus is unique in the C–C bond formation through laccase-catalyzed couplings of phenolic radicals.¹³ Interestingly, the *D. eschscholzii* genome contains an unclustered aldolase gene under the number 5476 (*aldoTL*, GenBank accession code: KP999992). Bioinformatic analysis

showed that this fungal aldolase has an 85% amino acid sequence similarity with its closest counterpart from *Aspergillus oryzae*.¹⁴ In many organisms, aldolases generally catalyze the C–C bond formations during the biosynthesis of structurally diverse natural products, and this family of enzymes can be further grouped into types I (predominant in plants and animals) and II aldolases (present in microorganisms).¹ We were therefore curious about whether the *aldoTL* coded aldolase could be used for the generation of alkaloid(s) with new skeleton(s) and of biological significance. To enable *D. eschscholzii* to produce alkaloids, a nitrogen-bearing precursor should be added in the fungal culture. Thus, a collection of low-molecular-weight nitrogenated compounds (Table S1) was assayed for appropriate 'alkaloid-imprinting' molecule(s) to start the present mycosynthetic endeavor. As a result, indole-3-carbinol (I3C, **1**) was selected and supplemented in the fungal culture since the supplementation of **1** in fungal culture led to the substantial change in the color of fermentation liquor (Figure S1). Moreover, our priority to supplement **1** in the fungal cultivation was intensified by the previous description of I3C as the precursor for 3,3'-diindolylmethane (DIM, **7**) at the phase I clinical trial.¹⁵ As detailed in this letter, I3C can be transformed by *D. eschscholzii* into dalesindole (**2**), an antibacterial and anti-inflammatory indole alkaloid with a new carbon skeleton, and the mechanism underlying the biochemical process has been clarified by a combination of gene knockout, intermediate capture, and genome implied enzyme inhibition (GIEI) approaches. Furthermore, dalesindole (**2a**)

Received: March 29, 2015

Published: May 18, 2015

tends to isomerize via a retro-Michael reaction to give three more stereoisomers (**2b–2d**), all retaining the bioactivity.

Repeated fractionation of the extract derived from the I3C-exposed fungal culture gave **2** in an isolated yield of 0.09% (Supporting Information), which was evidenced to have a molecular formula of $C_{27}H_{22}N_2O_3$ from the Na^+ -liganded molecular ion at m/z 445.1523 ($C_{27}H_{22}N_2O_3Na$ requires 445.1526) in its high-resolution electrospray ionization mass spectrometry (HR-ESI-MS). In its 1H NMR spectrum, the two 3-substituted indole motifs were indicated by a pair of broadened NH singlets at δ_H 10.01 and 10.21, which showed clear couplings with H-2' and H-2'' doublets at δ_H 7.56 ($J = 1.8$ Hz) and 7.38 ($J = 2.4$ Hz), respectively (Table S2). Furthermore, 1,2,3-trisubstituted benzene protons resonated at δ_H 6.38 (dd, $J = 8.4, 0.6$ Hz), 7.46 (t, $J = 8.4$ Hz), and 6.48 (dd, $J = 8.4, 0.6$ Hz). This observation, along with a broadened singlet at δ_H 11.30, highlighted the presence of a 2,3-disubstituted 5-hydroxychroman-4-one moiety with its non-aromatic proton resonances at δ_H 1.39 (3H, d, $J = 7.0$ Hz), 4.84 (1H, qd, $J = 6.6, 2.0$ Hz), and 3.56 (1H, dd, $J = 10.2, 2.0$ Hz). The proposal was substantiated by its 1H – 1H COSY, HMQC, and HMBC spectra, which allowed the unambiguous assignment of all 1H and ^{13}C NMR data of **2** (Figures 1 and S4–S14;

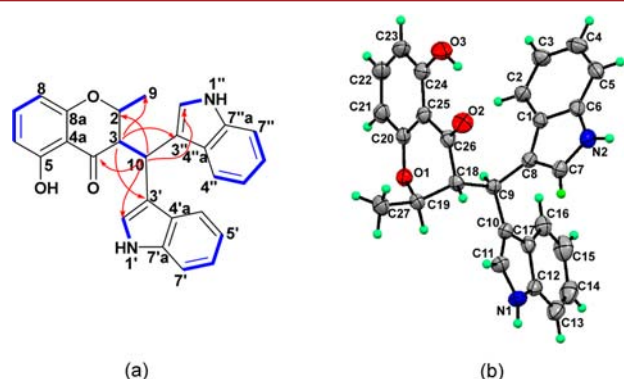


Figure 1. Key HMBC (red arrow) and 1H – 1H COSY correlations (blue bond) of **2** (a) with its structure confirmed by single crystal X-ray diffraction (b).

Table S2). In particular, the connection of chroman-4-one with two indole motifs was required by the HMBC correlations of H-3 (δ_H 3.56) with C-3'/3'' (δ_C 116.6/117.1) and C-9 (δ_C 18.1), and those of H-10 with C-2 (δ_C 76.3), C-2'/2'' (δ_C 124.0/124.1), and C-4 (201.1) (Figures 1 and S11–S12). The structure proposed for **2** was confirmed by single-crystal X-ray diffraction (Figure 1b; Table S3) using the anomalous dispersion of Cu $K\alpha$ radiation.

However, the crystal of **2** was shown to be a racemic mixture by its space group (Cc) and Flack parameter [0.4(6)] (Table S3). Chiral HPLC separation of **2** afforded enantiomers **2a** and **2b** (Figure S3), which resonated identically in their 1H and ^{13}C NMR spectra (Figures S6–S7). To address the absolute stereochemistry, electronic circular dichroism (ECD) spectra of all optional stereoisomers of **2** were calculated using quantum mechanical time-dependent density functional theory (TD-DFT),¹⁶ and the recorded CD curves of **2a** and **2b** were matches for those calculated for (2*S*,3*S*)-**2** and (2*R*,3*R*)-**2**, respectively (Figure 2).

Surprisingly, the chiral resolution of **2** led to the appearance of two more minor peaks (**2c** and **2d**) in the HPLC chromatograph (Figure S3). Subsequent chiral HPLC prepara-

tion was repeated to obtain sufficient materials of **2c** and **2d** to clarify their structures. Compounds **2c** and **2d** were identical in their ESI-MS, 1H and ^{13}C NMR spectra (Table S2 and Supporting Information). However, their 1H NMR spectra differed from those of **2a** and **2b** (Figure S6), suggesting that they could be diastereoisomers of **2a** and **2b**. The assumption was confirmed by the CD spectra of **2c** and **2d**, which resembled those calculated with (2*R*,3*S*)- and (2*S*,3*R*)-configurations, respectively (Figure 2). Moreover, the proposed absolute configurations of **2a–2d** agreed with the anticipated ROESY correlations (Figures S15–S16). The cocharacterization of diastereoisomers **2a–2d** suggested that they might be interchangeable via retro-Michael reaction (Figure 2). To evaluate the stereoselectivity of the aldolase-catalyzed coupling, the dalesindole (**2**) production was monitored kinetically by the chiral HPLC analysis using stereochemically defined enantiomers **2a–2d** as robust controls. Compound **2a** appeared on the eighth day of fermentation, but none of **2b–2d** could be detected even on the 12th day of the fungal cultivation (Figure S2). Thus, the aldolase-catalyzed reaction afforded stereoselectively **2a** whereas **2b–2d** were formed during the fractionation procedure via a retro-Michael reaction (Figure 2).

We next expanded our investigation to the mycosynthetic process toward **2**. As illustrated in Scheme 1, the starting chemical I3C (**1**) might be successively oxidized into indole-3-carboxaldehyde (**1A**, **3**) and indole-3-carboxylic acid (**1CA**, **4**). In the presence of acid, compound **4** could exist as a salt (**5**) which reacted with **3** to give the intermediate **6**. This intermediate might undergo a decarboxylative Claisen condensation to form **7**, which could conjugate with the fungal polyketide **8** to afford **2a** through Michael reaction. To confirm the assumption, the fungal growth was scaled-up with exposure to **1**, and the ethyl acetate extract was subjected to an LC-MS guided fractionation to give compounds **3**, **4**, **7**, and **8**. Moreover, bis(1*H*-indol-3-yl)methanone (**9**) was also isolated as a shunt product derived from intermediate **6**. The structure identification of **3** and **4** were characterized by the LC-MS comparison with authentic samples. Compounds **7–9** were isolated and identified according to the reported spectral data (Supporting Information),¹⁷ and the structure of **7** was confirmed by its single crystal X-ray diffraction (Table S4). Following the structural identification, the intermediates **3**, **4**, and **7** were separately supplemented as the exclusive sole indole source in *D. eschscholzii* cultures. As anticipated, compound **2** was detected in all extracts derived from the cultures exposed to each of those intermediates (Figure S17).

To reinforce the proposed cascade of reactions constructing **2**, a set of *in vitro* enzyme assays was conducted. As hypothesized, compounds **3**, **4**, and **7** were formed upon exposure of **1** to the intracellular protein derived from *D. eschscholzii* cells. However, the transformation of **1** into **3** was shown to be auto-oxidative as well since **3** could be detected in the aerated buffer. But, the conversion of **3** to **4** was found to be enzyme-dependent and catalyzed by the monooxygenase which was typically inhibited by its exposure to Ag^+ (2 mM) and Al^{3+} (1 mM) (Figure S18).¹⁸ Surprisingly, such an experimentation procedure gave a detectable amount of dalesindole (**2**). This could be due to the residual presence of **8** in the fungal cell protein fraction. To clarify the ambiguity, the intracellular protein was permeated against dialysis bag (MD 31) to remove all small molecules. Retreatment of **1** with the permeated protein yielded **3**, **4**, and **7**, but not **2**. This was reinforced by the production of **2** by the simultaneous exposure of **1** and **8** to

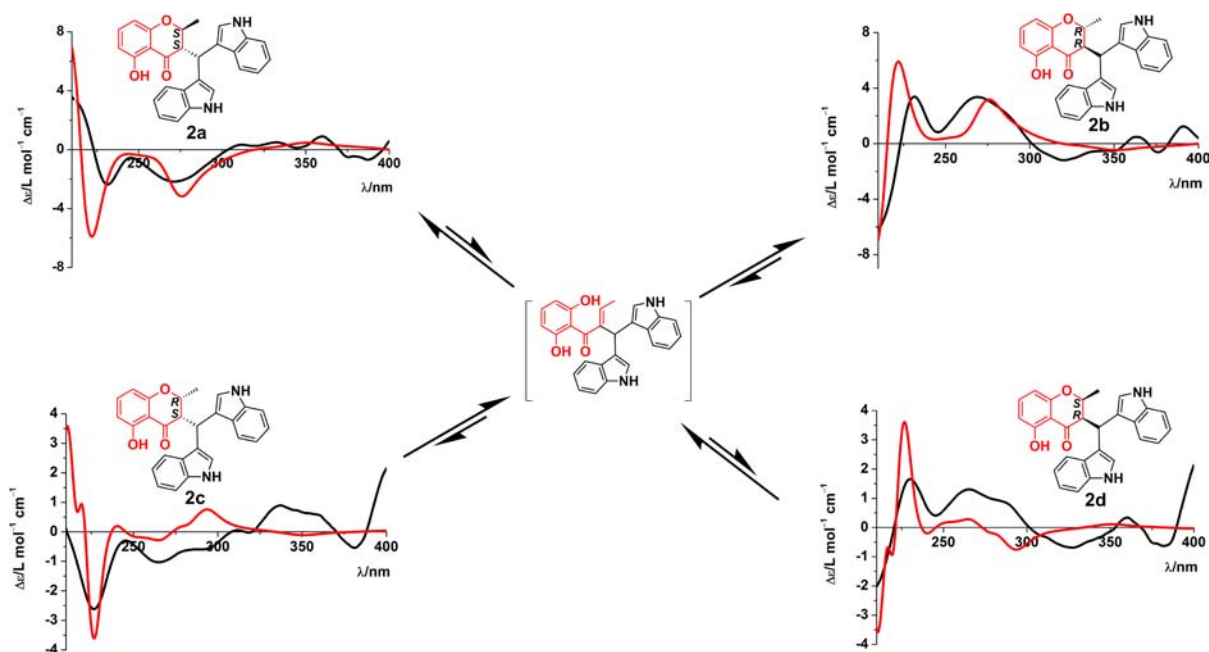
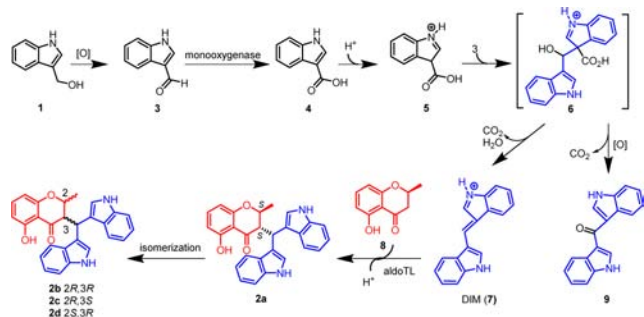


Figure 2. Stereochemical assignment of dalesindole (**2a**) and its diastereoisomers (**2b–2d**) formed via retro-Michael reaction. The calculated and experimental ECD spectra given in red and black, respectively.

Scheme 1. Generation and Isomerization of Dalesindole (2a) in the I3C-Exposed *D. eschscholzii* Culture



the permeated protein (Figure S19). These experiments confirmed that both **1** and **8** were essential precursors for the dalesindole (**2**) production.

The fungus was recultured with separate exposures to 8-amino-7-oxononanoate synthase (AONS) inhibitors, *D*-cycloserine,¹⁹ plumbagin,¹⁹ and triphenyltin acetate.²⁰ The ethyl acetate extracts derived from these AONS inhibitor supplemented fermentations were analyzed by LC-MS. As assumed, cosupplementation of **1** with any of the three AONS inhibitors (2.0 mM) in *D. eschscholzii* cultures substantially abolished or attenuated the production of **2** and **7** (Figure S20). These findings collectively indicated that the fungal AONS is involved in the fungal generation of **2** (Figure S20).

To address whether the coupling of **7** with the fungal chromone (**8**) was catalyzed by the class II aldolase (aldoTL) encoded by an unclustered *aldoTL* gene in the *D. eschscholzii* genome, the hygromycin resistance gene (*hph*) was used as a selection mark to knock out *aldoTL* to get the expected mutant (*aldoTLKO*) strain (Table S5; Figure S21). Subsequent LC-MS analysis was performed with the extracts derived from the cultures of wild type (WT) and *aldoTLKO* strains. Unlike the WT strain capable of generating **2**, **7**, and **8** in the presence of **1**, the I3C (**1**) exposed culture of the *aldoTLKO* strain was

unable to generate **2** despite its coproduction of **7** and **8**. Accordingly, the *aldoTL* of *D. eschscholzii* catalyzes the coupling reaction between **7** and **8** (Figure S22).

In view of the growing threat of human pathogenic bacteria,^{11,19} dalesindole (**2a**) and its stereoisomers (**2b–2d**) were tested for antibacterial activity using the MTT method.¹⁹ Compounds **2a**, **2b**, and **2d** exhibited broad and good potency against clinically isolated bacterial strains *Clostridium difficile*, *Veillonella* sp., *Prevotella buccae*, *Bacteroides fragilis*, and *Peptostreptococcus* sp. with IC₅₀ values of 5.0 μM, respectively, and **2c** showed selective inhibitions against *C. difficile* and *Veillonella* sp. (IC₅₀ values: 5 μM; Table S6). These alkaloids were also evidenced to regulate the TLR4 signaling pathway from the inhibition on IL-6 secretion from RAW264.7 cells by **2a** (34.8 ± 0.76%) and **2b** (39.2 ± 3.72%), which were comparable to the positive control (dexamethasone, 59.3 ± 1.96%) (Table S7). Thus, **2a** and **2b** possess anti-inflammatory activity as well.

Alkaloids seem more probable to be bioactive or lead molecules,¹⁰ but no nitrogenated secondary metabolite could be found in the culture of *D. eschscholzii*, an efficient polyketide producer.^{10,12} Recently some fungal oligoketides have been shown to couple with nitrogen-containing nonmicrobial small molecules to form a collection of “unnatural” or “designed” alkaloids through radical coupling^{10,13} and Pictet–Spengler reaction.¹¹ Mechanistically distinct from the observations, this work describes the exploitation of an unclustered aldolase gene in the *D. eschscholzii* genome to generate (2*S*,3*S*)-dalesindole (**2a**), a skeletally new polyketide-alkaloid hybrid molecule with antibacterial and anti-inflammatory activities. As suggested by the fungal genome, this hybridization is facilitated by the class II aldolase which catalyzes the coupling of fungal chromone with DIM formed *in situ* from I3C in the presence of monooxygenase and 8-amino-7-oxononanoate synthase. Steered by the steric hindrance, (2*S*,3*S*)-dalesindole (**2a**) isomerizes via a retro-Michael reaction to give a major (**2b**) and two minor stereoisomers (**2c** and **2d**), which are also

bioactive. The work exemplifies bioactive hybrid formations by the in-culture coupling of fungal oligoketide with the structurally unpredictable metabolite produced through fungal transformation of the supplemented exogenous small molecules, and the new natural product-like compounds therefrom might have higher probability to be bioactive or lead molecules desired by the current drug discovery pipeline.

■ ASSOCIATED CONTENT

■ Supporting Information

Complete description of methods, additional tables, and figures, including full NMR data and crystallographic data. The Supporting Information is available free of charge on the ACS Publications website at DOI: 10.1021/acs.orglett.5b00882.

■ AUTHOR INFORMATION

Corresponding Author

*E-mail: rxtan@nju.edu.cn.

Notes

The authors declare no competing financial interest.

■ ACKNOWLEDGMENTS

This work was cofinanced by the MOST (2013AA092901) and NSFC grants (81421091, 91413120, and 21132004) and the Natural Science Foundation of Jiangsu Province (BK2012378).

■ REFERENCES

- (1) Brovetto, M.; Gamenara, D.; Méndez, P. S.; Seoane, G. A. *Chem. Rev.* **2011**, *111*, 4346–4403.
- (2) Samland, A. K.; Sprenger, G. A. *Appl. Microbiol. Biotechnol.* **2006**, *71*, 253–264.
- (3) Abdelmohsen, U. R.; Bayer, K.; Hentschel, U. *Nat. Prod. Rep.* **2014**, *31*, 381–399.
- (4) Hertweck, C. *Angew. Chem., Int. Ed.* **2009**, *48*, 4688–4716.
- (5) Xu, W.; Gavia, D. J.; Tang, Y. *Nat. Prod. Rep.* **2014**, *31*, 1474–1487.
- (6) Kittakoop, P.; Mahidol, C.; Ruchirawat, S. *Curr. Top. Med. Chem.* **2014**, *14*, 239–252.
- (7) Gritsch, P. J.; Leitner, C.; Pfaffenbach, M.; Gaich, T. *Angew. Chem., Int. Ed.* **2014**, *53*, 1208–1217.
- (8) Dhakshinamoorthy, A.; Garcia, H. *Chem. Soc. Rev.* **2014**, *43*, 5750–5765.
- (9) Ge, H. M.; Yan, W.; Guo, Z. K.; Luo, Q.; Feng, R.; Zang, L. Y.; Shen, Y.; Jiao, R. H.; Xu, Q.; Tan, R. X. *Chem. Commun.* **2011**, *47*, 2321–2323.
- (10) Tian, Y.; Jiang, N.; Zhang, A. H.; Chen, C. J.; Deng, X. Z.; Zhang, W. J.; Tan, R. X. *Org. Lett.* **2015**, *17*, 1457–1460.
- (11) Yan, W.; Ge, H. M.; Wang, G.; Jiang, N.; Mei, Y. N.; Jiang, R.; Li, S. J.; Chen, C. J.; Jiao, R. H.; Xu, Q.; Ng, S. W.; Tan, R. X. *Proc. Natl. Acad. Sci. U.S.A.* **2014**, *111*, 18138–18143.
- (12) (a) Zhang, Y. L.; Ge, H. M.; Zhao, W.; Dong, H.; Xu, Q.; Li, S. H.; Li, J.; Zhang, J.; Song, Y. C.; Tan, R. X. *Angew. Chem., Int. Ed.* **2008**, *47*, 5823–5826. (b) Zhang, Y. L.; Zhang, J.; Jiang, N.; Lu, Y. H.; Wang, L.; Xu, S. H.; Wang, W.; Zhang, G. F.; Xu, Q.; Ge, H. M.; Ma, J.; Song, Y. C.; Tan, R. X. *J. Am. Chem. Soc.* **2011**, *133*, 5931–5940.
- (13) Fang, W.; Ji, S.; Jiang, N.; Wang, W.; Zhao, G. Y.; Zhang, S.; Ge, H. M.; Xu, Q.; Zhang, A. H.; Zhang, Y. L.; Song, Y. C.; Zhang, J.; Tan, R. X. *Nat. Commun.* **2012**, *3*, 1039.
- (14) Elshafei, A. M.; Elsayed, M. A.; Abdel-Fatah, O. M.; Ali, N. H.; Mohamed, L. A. *J. Basic Microb.* **2005**, *45*, 31–40 and related references therein.
- (15) Banerjee, S.; Kong, D.; Wang, Z.; Bao, B.; Hillman, G. G.; Sarkar, F. H. *Mutat. Res.* **2011**, *728*, 47–66.

- (16) Wu, Q.; Jiang, N.; Han, W. B.; Mei, Y. N.; Ge, H. M.; Guo, Z. K.; Weng, N. S.; Tan, R. X. *Org. Biomol. Chem.* **2014**, *12*, 9405–9412.
- (17) (a) Sutapa, R.; Rahul, G.; Madhumita, M.; Churala, P.; Arumugam, M.; Joydeep, M.; Parasuraman. *J. Med. Chem. Res.* **2014**, *23*, 1371–1377. (b) Gong, Q. F.; Zhang, Y. M.; Tan, N. H.; Chen, Z. H. *Zhongguo Zhong yao za zhi.* **2008**, *33*, 1269–1272. (c) Guchhait, S. K.; Kashyap, M.; Kamble, H. J. *Org. Chem.* **2011**, *76*, 4753–4758.
- (18) Chen, S. H.; Lin, Q. S.; Xiao, Y.; Deng, Y. Y.; Chang, C. Q.; Zhong, G. H.; Hu, M. Y.; Zhang, L. H. *PLoS One* **2013**, *8*, 1–9.
- (19) Han, W. B.; Lu, Y. H.; Zhang, A. H.; Zhang, G. F.; Mei, Y. N.; Jiang, N.; Lei, X.; Song, Y. C.; Ng, S. W.; Tan, R. X. *Org. Lett.* **2014**, *16*, 5366–5369.
- (20) Hwang, I. T.; Choi, J. S.; Song, H. Y.; Cho, S. J.; Lim, H. K.; Park, N. J.; Lee, D. H. *Pestic. Biochem. Physiol.* **2010**, *97*, 24–31.